Chiral Supramolecular liquid crystal based on pillararene and its application in information encryption

Bicong Liang,[a] Yujie Cheng,[b] Jiaxin Ma,[b] Lan Jia,[a] Qiang Zheng,[a] Pi Wang*[a] and Danyu Xia*[b]

[a]*College of Materials Science and Engineering, Taiyuan University of Technology, Taiyuan, 030024, P. R. China. E-mail: wangpi@tyut.edu.cn.*

[b]*Scientific Instrument Center, Shanxi University, Taiyuan 030006, P. R. China. Email: danyuxia@sxu.edu.cn.*

Electronic Supplementary Information (10 pages)

1. Materials and methods

All chemicals were obtained from commercial suppliers and were used as supplied without further purification. All reactions were conducted with oven-dried glassware under atmosphere or nitrogen. Solvents were dried and distilled following usual protocols. Column chromatography was carried out using silica gel (200-300 mesh). Compounds **P5-Chol**[S1] and **TPE-CN**[S2] was prepared according to published procedures. The NMR spectra were recorded with a Bruker Avance DMX 600 spectrophotometer. High-resolution mass spectrometry experiments were performed with a Thermo Scientific Q Exactive instrument. The melting points were collected on a SGW X-4 automatic melting point apparatus. Scanning Electron Microscopy (SEM) investigations were carried out on a PerkinElmer Gemini SEM300 instrument. Fluorescent microscopy investigations were carried out on a HITACHI F-7100 fluorescence spectrometer. Phase behavior was studied by NP900 Polarizing Optical Microscopy (POM) equipped with a hot-stage from -40.0 to 500 °C. Room-temperature X-ray Diffraction (XRD) experiments were performed on a Bruker D2 PHASER X-ray diffractometer using Cu $K_{\alpha 1}$ radiation. Circular dichroism (CD) spectra were performed on a Bio-Logic MOS-500 instrument.

2. Host−guest complexation study of P5-Chol and TPE-CN

As shown in Fig. S1, compared to **P5-Chol** and **TPE-CN** alone (Fig. S1a and c), the peaks related to the protons H_4−H_6 of the alkyl chain group on **TPE-CN** shifted upfield, and the peaks related to the protons H_f−H_h and H_o−H_q on **P5-Chol** shifted downfield, indicating that the alkyl chain part of **TPE-CN** are located within the cavity of **P5-Chol** upon the formation of the host−guest inclusion complex **P5-Chol⊃TPE-CN**.

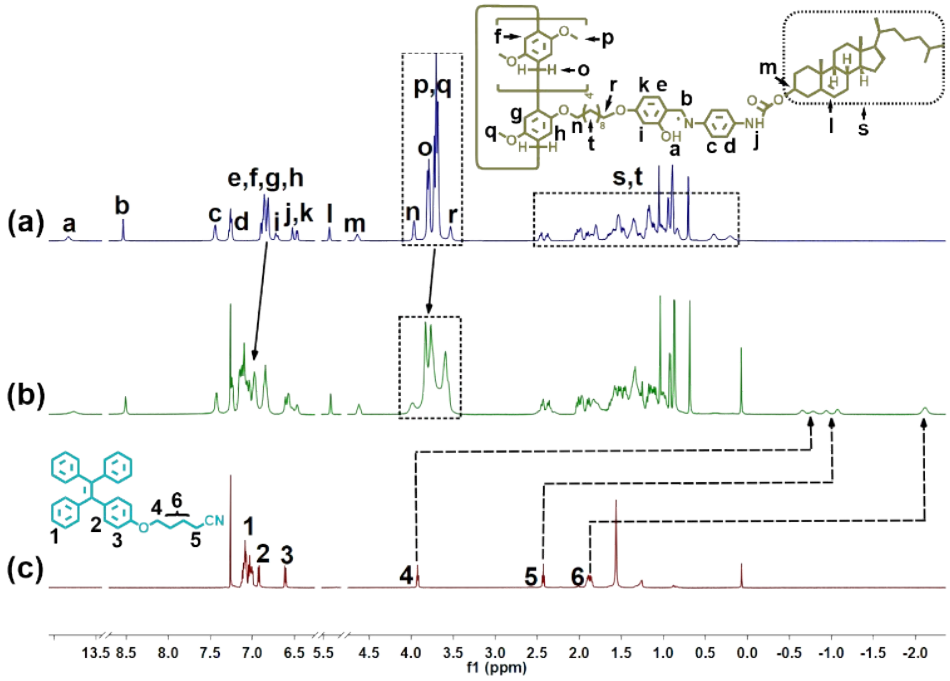

Figure S1. Partial ^{1}H NMR spectra (600 MHz, $CDCl_3$, 298 K): (a) **P5-Chol** (5.00 mM); (b) **P5-Chol** (5.00 mM) and **TPE-CN** (5.00 mM); (c) **TPE-CN** (5.00 mM).

3. ^{1}H NMR spectroscopy of P5-Chol and TPE-CN at different concentrations

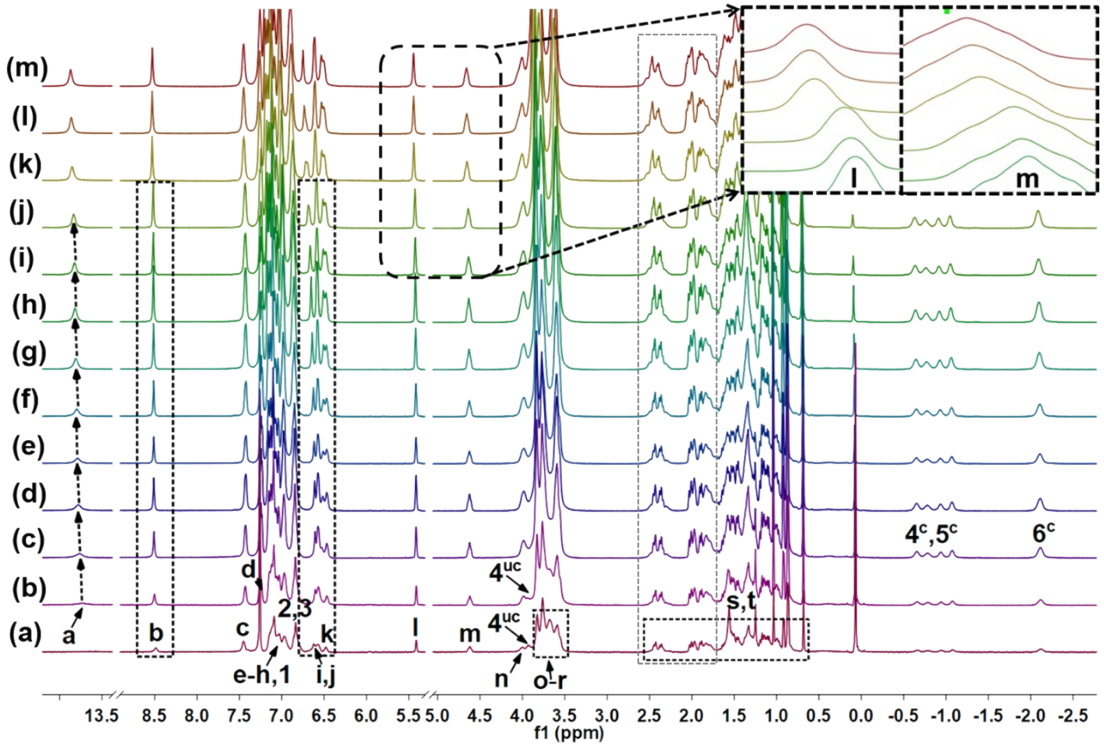

Figure S2. Partial ^{1}H NMR spectra (600 MHz, $CDCl_3$, 298 K) of equimolar mixtures of **P5-Chol** and **TPE-CN** at different concentrations: (a) 2.50 mM; (b) 5.00 mM; (c) 10.0 mM; (d) 14.28 mM; (e) 20.0 mM; (f) 25.0 mM; (g) 33.3 mM; (h) 40.0 mM; (i) 50.0 mM; (j) 62.5 mM; (k) 70.0 mM; (l) 83.3 mM; (m) 100 mM.

4. Partial X-ray diffraction patterns of P5-Chol and P5-Chol⊃TPE-CN at room temperature

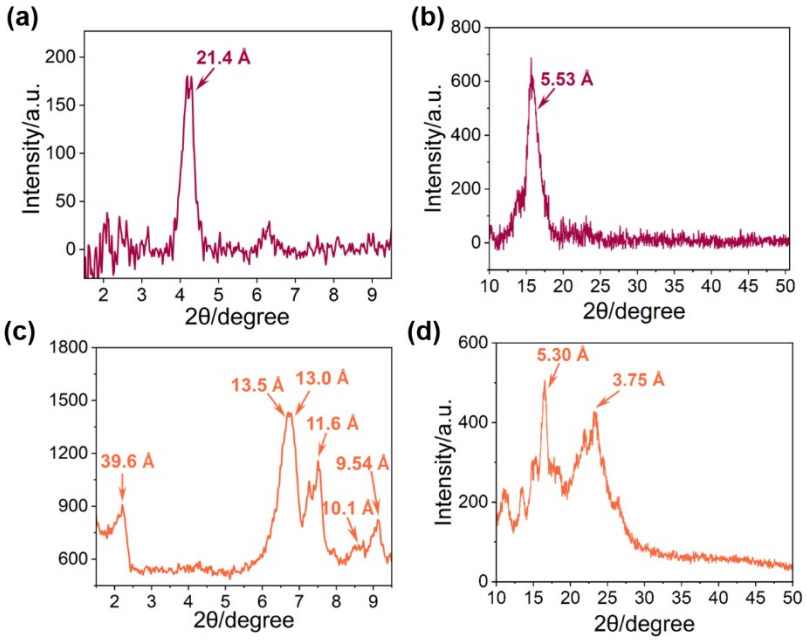

Figure S3. (a) Partial XRD pattern of **P5-Chol** at room temperature in the small-angle range; (b) Partial XRD pattern of **P5-Chol** at room temperature in the wide-angle range; (c) Partial XRD pattern of **P5-Chol⊃TPE-CN** at room temperature in the small-angle range; (d) Partial XRD pattern of **P5-Chol⊃TPE-CN** at room temperature in the wide-angle range.

5. Calculated structures of P5-Chol and TPE-CN

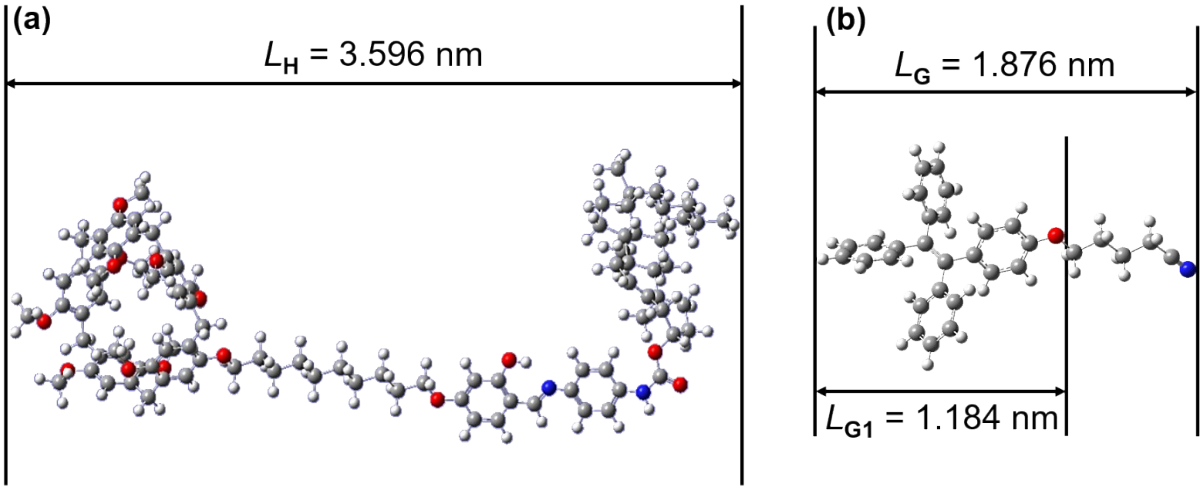

Figure S4. Calculated structures: (a) **P5-Chol**; (b) **TPE-CN.**

*6. SEM images of **P5-Chol** and **P5-Chol⊃TPE-CN***

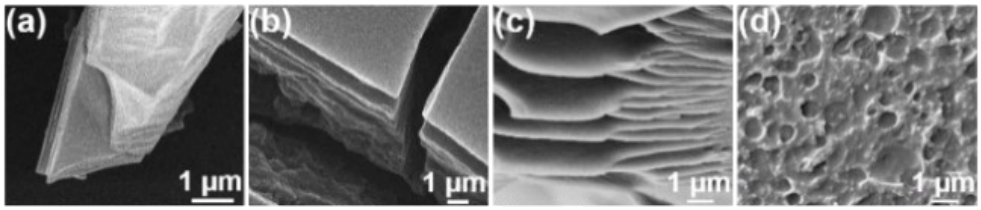

Figure S5. SEM images of gold-coated samples: (a) **P5-Chol** (70.0 mM) (lamellar phase); (b) **P5-Chol** (70.0 mM) and **TPE-CN** (70.0 mM) (lamellar phase); (c) **P5-Chol** (70.0 mM) and **TPE-CN** (70.0 mM) (intermediate state); (d) **P5-Chol** (70.0 mM) and **TPE-CN** (70.0 mM) (bicontinuous cubic phase).

7. Circular dichroism (CD) spectra experiments of P5-Chol and P5-Chol⊃TPE-CN

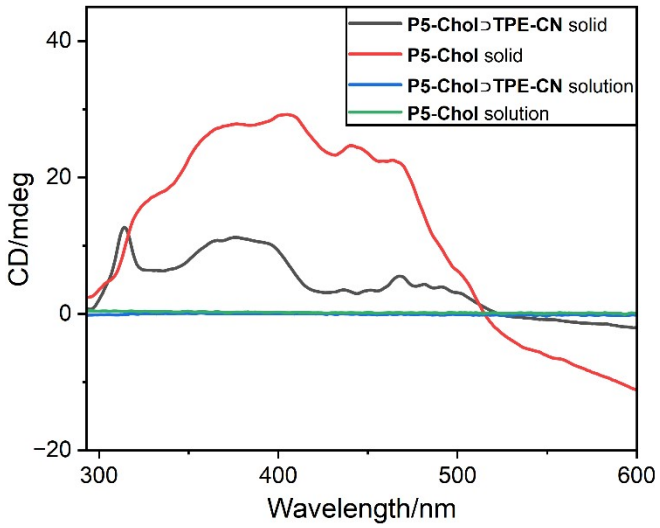

Figure S6. CD spectra of **P5-Chol⊃TPE-CN** in the solid state (black line), **P5-Chol** in the solid state (red line), **P5-Chol⊃TPE-CN** in solution (10^{-2} mM, blue line) and **P5-Chol** in solution (10^{-2} mM, green line).

8. ^{1}H NMR spectroscopy experiments of the pH-responsiveness of P5-Chol⊃TPE-CN

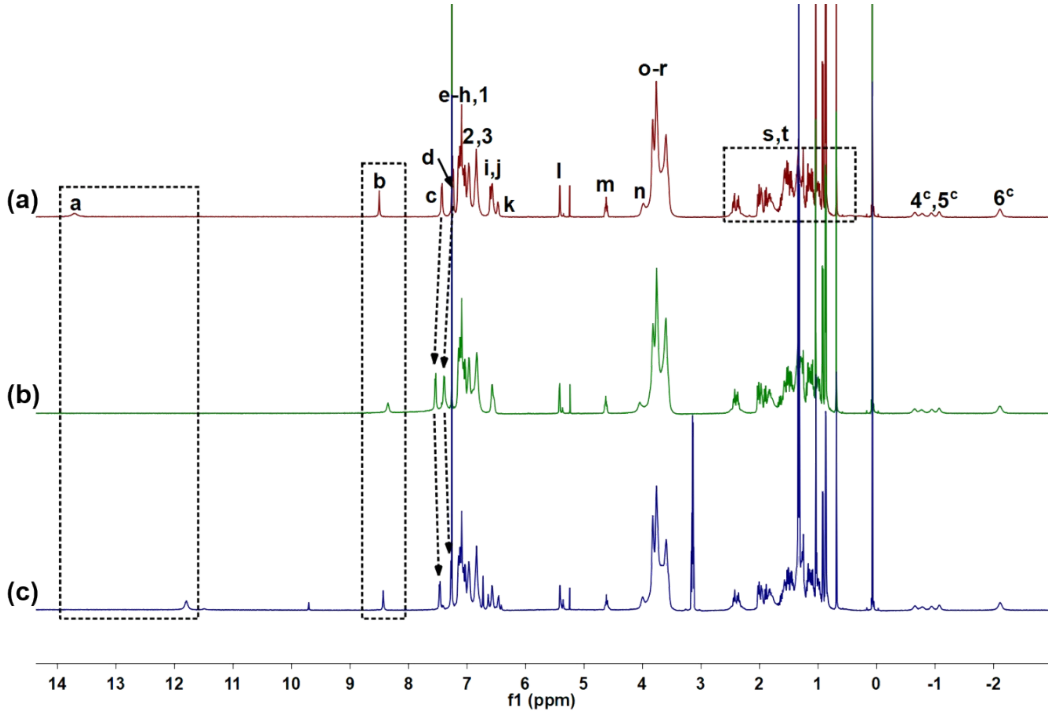

Figure S7. Partial ^{1}H NMR spectra (600 MH, $CDCl_3$, room temperature): (a) **P5-Chol** (5.00 mM) and **TPE-CN** (5.00 mM); (b) After addition of 2.0 molar equiv. of TFA to a; (c) After further addition of 4.0 molar equiv. of TEA to b.

9. POM images of P5-Chol during the decrease of temperature at the concentration of 10 mM

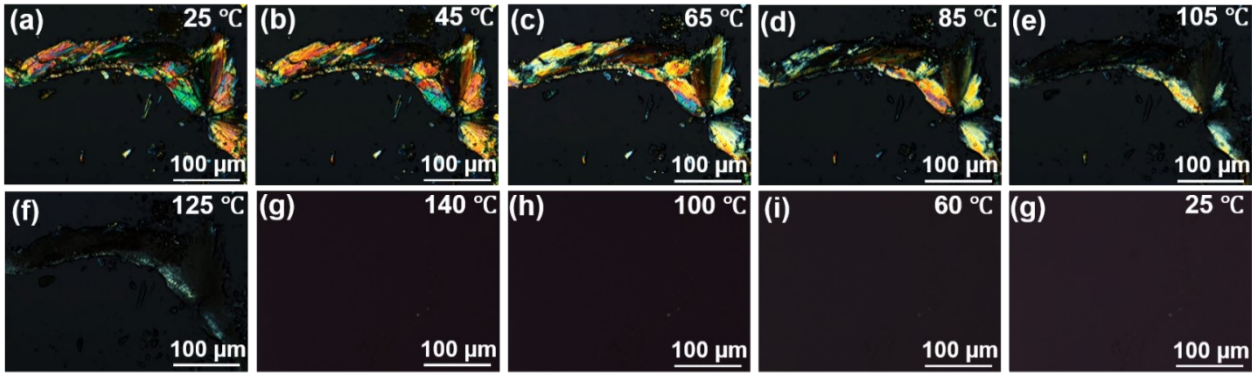

Fig. S8 Polarized optical micrograph (POM) of **P5-Chol** at different temperatures: (a) 25.0 ℃; (b) 45.0 ℃; (c) 65.0 ℃; (d) 85 ℃; (e) 105 ℃; (f) 125 ℃; (g) 140 ℃; (h) when the temperature of **P5-Chol** increased to 140 ℃ and then decreased to 100 ℃ ; (i) 60 ℃; (g) 25 ℃.

10. POM images of P5-Chol during the decrease of temperature at the concentration of 70 mM

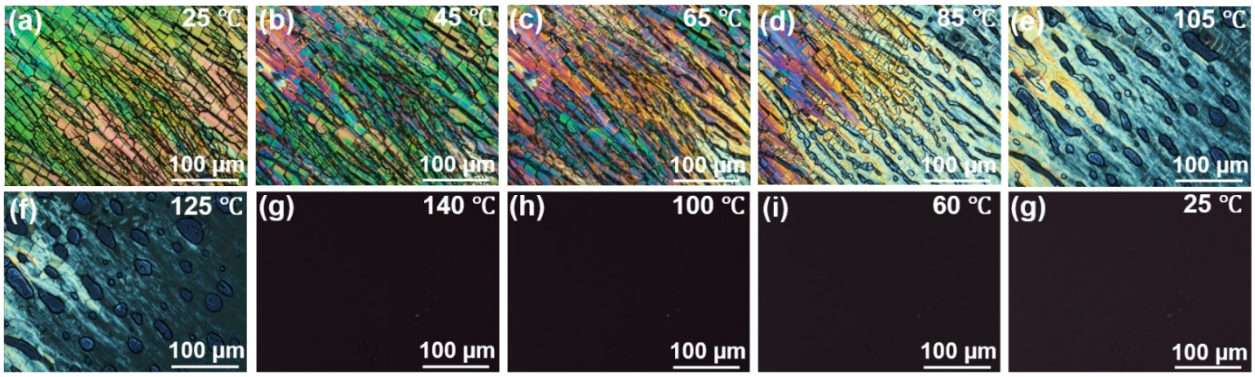

Fig. S9 Polarized optical micrograph (POM) of **P5-Chol** at different temperatures: (a) 25.0 ℃; (b) 45.0 ℃; (c) 65.0 ℃; (d) 85 ℃; (e) 105 ℃; (f) 125 ℃; (g) 140 ℃; (h) when the temperature of **P5-Chol** increased to 140 ℃ and then decreased to 100 ℃ ; (i) 60 ℃; (g) 25 ℃.

11. POM images of P5-Chol⊃TPE-CN during the decrease of temperature at the concentration of 10 mM

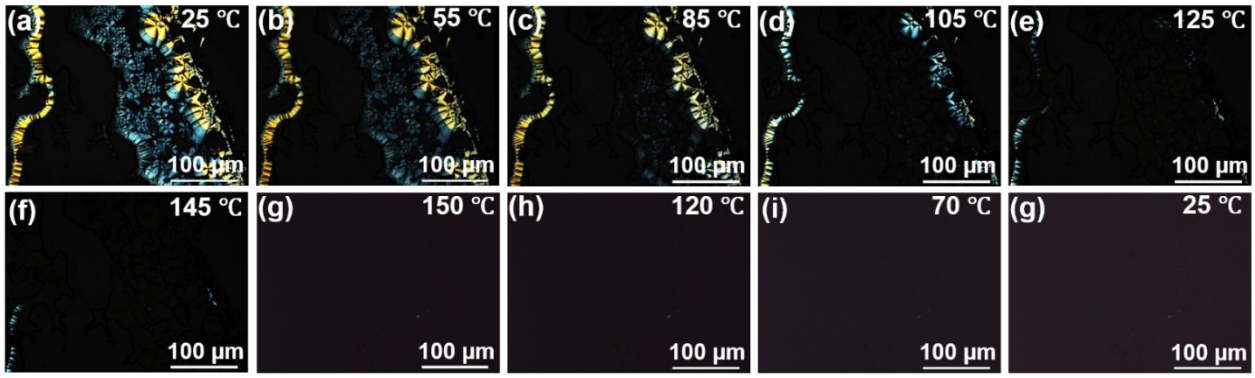

Fig. S10 Polarized optical micrograph (POM) of **P5-Chol⊃TPE-CN** at different temperatures: (a) 25.0 ℃; (b) 55.0 ℃; (c) 85.0 ℃; (d) 105 ℃; (e) 125 ℃; (f) 145 ℃; (g) 150 ℃; (h) when the temperature of **P5-Chol⊃TPE-CN** increased to 150 ℃ and then decreased to 120 ℃ ; (i) 70 ℃; (g) 25 ℃.

12. POM images of P5-Chol⊃TPE-CN during the decrease of temperature at the concentration of 70 mM

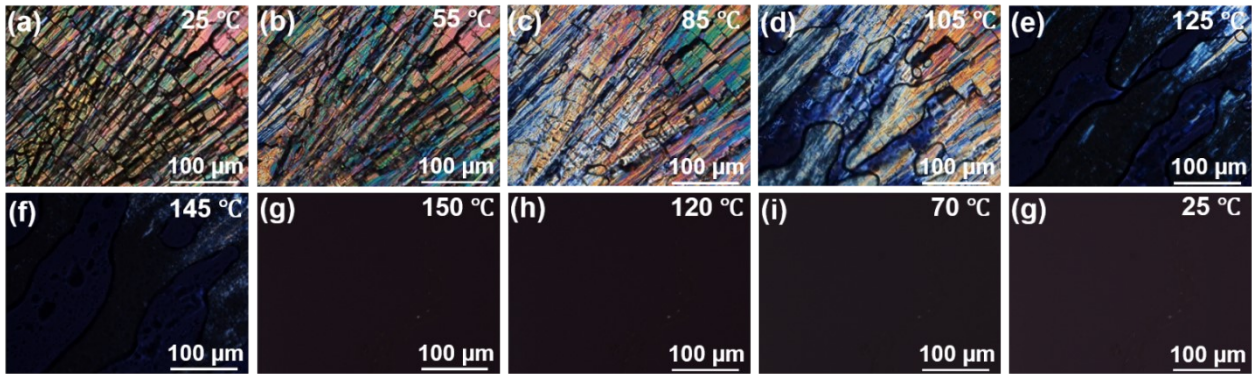

Fig. S11 Polarized optical micrograph (POM) of **P5-Chol⊃TPE-CN** at different temperatures: (a) 25.0 ℃; (b) 55.0 ℃; (c) 85.0 ℃; (d) 105 ℃; (e) 125 ℃; (f) 145 ℃; (g) 150 ℃; (h) when the temperature of **P5-Chol⊃TPE-CN** increased to 150 ℃ and then decreased to 120 ℃ ; (i) 70 ℃; (g) 25 ℃.

13. Absorption and emission spectra of P5-Chol and TPE-CN

The photophysical properties of **P5-Chol** and **TPE-CN** were investigated by UV-vis adsorption and fluorescence emission spectroscopy. There is no effective overlap between the absorption spectrum and fluorescence spectrum of **P5-Chol** and **TPE-CN**, indicating no effective fluorescence-resonance energy transfer (FRET) between them.

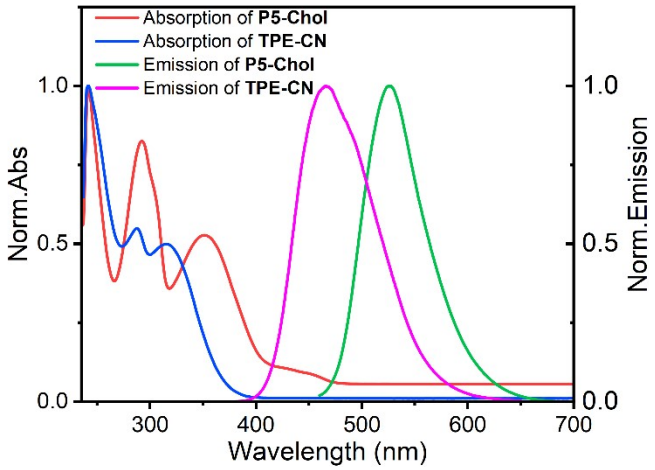

Fig. S12 Normalized absorption and emission spectra of **P5-Chol** (λ_{ex} = 360 nm) and **TPE-CN** (λ_{ex} = 315 nm) in the solid stated.

14. Solid fluorescence emission spectra of P5-Chol⊃TPE-CN

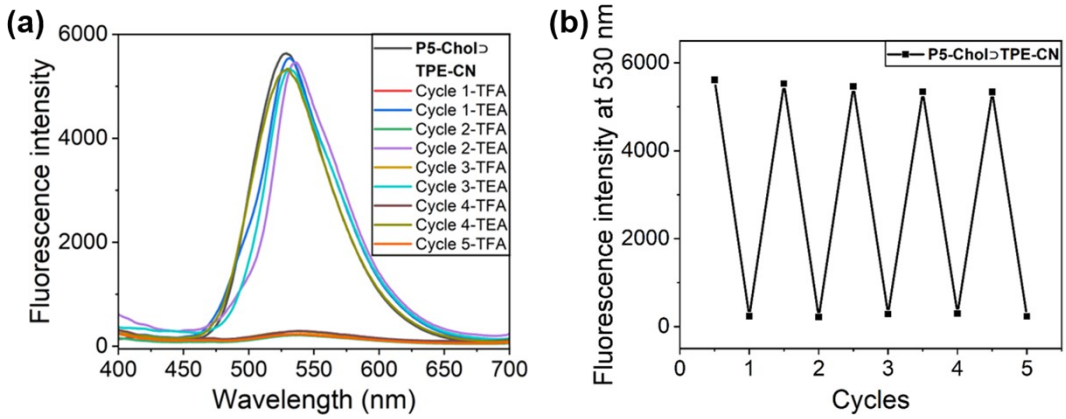

Fig. S13 (a) The solid fluorescence emission spectra of **P5-Chol⊃TPE-CN** in the solid state during five cycle experiments (λ_{ex} = 360 nm; λ_{em} = 530 nm); (b) The line chart of **P5-Chol⊃TPE-CN** during five cycle experiments.

References

S1. B. Liang, D. Xia, Y. Cheng, Q. Zheng and P. Wang, *A supramolecular polymer network constructed using a pillararene-based multi-functional monomer and its application as a rewritable fluorescent paper*, *Dalton Trans.*, 2023, **52**, 17099-17103.

S2. X. H. Wang, N. Song, W. Hou, C. Y. Wang, Y. Wang, J. Tang and Y. W. Yang, *Efficient Aggregation-Induced Emission Manipulated by Polymer Host Materials*, *Adv. Mater.*, 2019, **31**, 1903962.